

Relaxing Positional Alignment in Masked Diffusion Language Models

Mengyu Ye¹ Ryosuke Takahashi^{1,2} Keito Kudo^{1,2} Jun Suzuki^{1,2,3}

Abstract

Masked diffusion language models (MDLMs) have emerged as a promising alternative to dominant autoregressive approaches. Although they achieve competitive performance on several tasks, a substantial gap remains in open-ended text generation. We hypothesize that one cause of this gap is that strict positional prediction makes MDLM decoding highly sensitive to token misalignment, and we show through controlled interventions that a one-position shift can severely disrupt semantics. This observation suggests that enforcing strict positional supervision during training is misaligned with the irreversible denoising dynamics of MDLM decoding. Motivated by this mismatch, we adopt an alignment-flexible supervision strategy during fine-tuning. Specifically, we introduce a special token <SLACK> via the connectionist temporal classification objective. We apply this approach to the widely used MDLM and conduct experiments on five open-ended text generation benchmarks. Our method consistently outperforms the original model and improves robustness to positional shifts, indicating that relaxing strict positional supervision is an important factor in improving generation quality in MDLMs.

1. Introduction

Diffusion models have been applied to discrete data such as text (Sahoo et al., 2024; Arriola et al., 2025; Nie et al., 2025a; Zhu et al., 2025; Ye et al., 2025). Diffusion-based approaches support flexible token update orders, multi-token unmasking, bidirectional context modeling, and flexible conditioning. These properties make them an appealing alternative to standard language modeling with autoregressive language models (Vaswani et al., 2017; Brown et al., 2020).

Masked diffusion language models (MDLMs) are among

¹Tohoku University ²RIKEN ³NII LLMC. Correspondence to: Mengyu Ye <ye.mengyu.s1@dc.tohoku.ac.jp>, Jun Suzuki <is-failab-research@grp.tohoku.ac.jp>.

the most widely used diffusion-based approaches for text generation. Recent works such as the LLaDA family (Nie et al., 2025b; Zhu et al., 2025) have scaled MDLMs to 8B parameters, achieving performance comparable to similarly sized autoregressive models on several benchmarks. However, these evaluations have focused on tasks assessed using exact token- or string-level matching, such as GPQA (Rein et al., 2024), MMLU (Hendrycks et al., 2021b;a), and MBPP (Austin et al., 2021). In contrast, benchmarks requiring open-ended generation and coherent responses, such as Arena-Hard (Li et al., 2025b; 2024) and MTBench (Zheng et al., 2023), remain challenging for MDLMs. This discrepancy suggests, despite recent progress, open-ended text generation remains difficult for current MDLMs.

We argue that an overlooked limitation of MDLMs in open-ended generation, particularly under standard diffusion decoding settings as used by the LLaDA family, is sensitivity to token misalignment caused by strict positional alignment between target tokens and output positions. Text is often highly position-sensitive, and even a single misplaced token can severely disrupt semantic coherence. This issue is further exacerbated in typical MDLM decoding because once a token is unmasked, it is committed and cannot be revised. As a result, early local errors cannot be corrected and may persist across subsequent denoising steps, leading to global degradation in generation quality (Wang et al., 2025).

We empirically demonstrate that repeated one-position shift interventions during MDLM generation, despite preserving local token content, cause a substantial drop in generation quality on open-ended benchmarks. This suggests that a major source of error is not lexical choice, but rather that enforcing strict one-to-one positional supervision during training is misaligned with the irreversible nature of MDLM decoding.

Prior work has shown that positional misalignment can be harmful in settings where it is induced by task constraints, such as length-mismatched infilling (e.g., DDOT (Zhang et al., 2025a), DreamOn (Wu et al., 2025b)). In contrast, we show that positional misalignment can arise intrinsically during standard open-ended MDLM decoding, even when no explicit length or alignment mismatch is imposed.

To address this issue, we relax the strict requirement that each token must be generated at an exact position. Specifi-

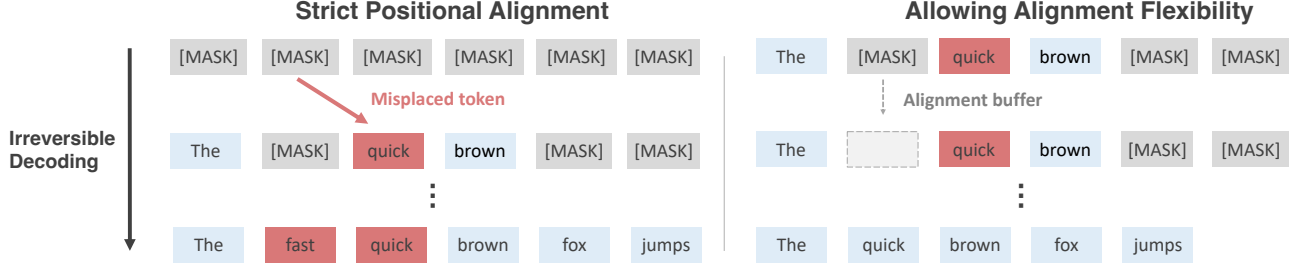


Figure 1. Under standard MDLM decoding, tokens are generated at fixed positions and become immutable once unmasked. A small position error early in decoding can therefore propagate through subsequent steps, leading to cascading semantic degradation (left). Allowing limited alignment flexibility introduces non-semantic buffer positions that absorb local misalignment, preventing error propagation while preserving the irreversible decoding process (right).

cally, we introduce an alignment-flexible sequence objective based on connectionist temporal classification (CTC), alongside the standard cross-entropy loss during supervised fine-tuning (SFT). This objective allows the model to produce an auxiliary $\langle \text{SLACK} \rangle$ token that absorbs positional uncertainty in the alignment between the target sequence and the model’s output positions. These tokens are removed after decoding and do not appear in the final output. We apply this training objective to a widely used MDLM, LLaDA-8B-Instruct. Across five open-ended text generation benchmarks, the resulting model consistently improves over both the original LLaDA-8B-Instruct and a matched baseline trained under identical settings.

Overall, this work makes three contributions. (i) We identify position-level alignment sensitivity as a key limitation of MDLMs for open-ended text generation. (ii) We show that adding an alignment-flexible auxiliary objective during SFT effectively relaxes positional constraints without altering the task interface. (iii) We show that this approach improves performance across five open-ended generation benchmarks and enhances robustness to positional misalignment.

2. Masked Diffusion Language Models

MDLMs define a probability distribution over sequences through a forward noising process and a learned reverse denoising process. Let $x_0 = (x_0^1, \dots, x_0^L)$ be a token sequence, whose length is L , and contain no masks. The forward process independently masks each token with a probability given by a strictly decreasing function $\alpha_t \in [0, 1]$ in t . Applying masks to the tokens with probability $1 - \alpha_t$ results in a partially masked sequence x_t . When $t = 1$, all tokens are masked; when $t = 0$, the sequence remains unchanged.

2.1. Training

Pre-training. The reverse process is parameterized by a mask predictor $P_\theta(\cdot | x_t)$, which takes the partially masked sequence x_t as input and predicts all masked tokens in par-

allel. Let the indicator $\mathbf{1}_{[x_t^i = M]}$ be 1 if the i -th token in x_t , namely x_t^i , is masked (represented by $x_t^i = M$), and 0 otherwise. Then, training proceeds by sampling t from a uniform distribution $\mathcal{U}[0, 1]$, i.e., $t \sim \mathcal{U}[0, 1]$, constructing x_t via the forward process, and minimizing a masked cross-entropy loss evaluated only at masked positions; thus, the pre-training objective is:

$$\mathcal{L}_{\theta, t}^{\text{CE}} \triangleq -\mathbb{E}_{t, x_0, x_t} \left[\gamma_t \sum_{i=1}^L \mathbf{1}_{[x_t^i = M]} \log P_\theta(x_0^i | x_t) \right], \quad (1)$$

where $\gamma_t = -\frac{\alpha'_t}{1 - \alpha_t}$, and α'_t represents the derivative of α_t with respect to t .¹

Supervised fine-tuning. SFT adapts a pre-trained MDLM to instruction-following using paired data (q_0, r_0) , where q_0 denotes the prompt and r_0 the corresponding response. The objective is to model the conditional distribution $P_\theta(r_0 | q_0)$. Similar to pre-training, each token in r_0 is independently masked with probability α_t , as explained above, a monotonically decreasing function of t , to obtain r_t , while q_0 is kept intact. The mask predictor conditions on the concatenation of q_0 and r_t to predict masked response tokens. We then redefine the pre-training objective shown in Eq. (1) as the SFT objective as follows:

$$\mathcal{L}_{\theta, t}^{\text{CE}} = -\mathbb{E}_{t, q_0, r_0, r_t} \left[\gamma_t \sum_{i=1}^{L_r} \mathbf{1}_{[r_t^i = M]} \psi_\theta(r_0^i, q_0, r_t) \right], \quad (2)$$

where L_r denotes the response length, and $\psi_\theta(r_0^i, q_0, r_t) = \log P_\theta(r_0^i | q_0, r_t)$.

Relation between pre-training and SFT. Eq. (2) can also cover the pre-training objective if we view pre-training input token sequences as never including a prompt part q_0 but only a response part; namely, q_0 is always an empty sequence and $x_t = r_t$.

¹See detailed explanation in Sahoo et al. (2024).

2.2. Inference

After training, text generation discretizes the reverse diffusion process to sample from the conditional distribution $P_\theta(r_0 \mid q_0)$. Following standard MDLM decoding (e.g., LLaDA), we fix the response length L_r as a hyperparameter and initialize generation of r_t at $t = 1$, yielding a fully masked response sequence, i.e.,

$$r_1 = (\langle \text{MASK} \rangle, \dots, \langle \text{MASK} \rangle) \in (\mathcal{V} \cup \{\langle \text{MASK} \rangle\})^{L_r}, \quad (3)$$

where \mathcal{V} denotes the model’s vocabulary. At an intermediate timestep t (from $t = 1$ to $t = 0$), all masked tokens are predicted simultaneously and independently. After prediction, a subset of the newly revealed tokens is re-masked at each step to ensure that the overall masking ratio follows the prescribed noise schedule. Following LLaDA, the low-confidence remasking (Chang et al., 2022) is adopted; tokens with lower prediction confidence are selected for re-masking, and tokens that remain unmasked are carried forward and not re-masked in subsequent steps, making this process irreversible.

3. Preliminary Experiments: Sensitivity to Positional Misalignment

MDLMs generate text by progressively revealing tokens at fixed sequence indices. Under standard decoding, once a token is unmasked, it remains fixed for the remainder of the generation. Prior work has shown that this irreversible decoding dynamic allows errors introduced early in generation to persist and accumulate (Wang et al., 2025).

This section studies positional misalignment as a source of accumulated error. Unlike token identity errors, an index-level misalignment can affect the interpretation of all subsequent tokens. Our goal is to isolate the effect of accumulated local positional misalignment under irreversible decoding, while keeping token identities and local content unchanged. We also observe shift-like local inconsistencies, such as short-range token duplication and character-level misalignment, in standard generations from LLaDA-8B-Instruct², further motivating the focus on positional misalignment.

To this end, we introduce a **controlled sequence shift intervention**. We then evaluate the intervention’s negative effect as a proxy for the negative effects of true positional misalignment that occur during decoding.

3.1. Controlled Sequence Shift Intervention

This section describes the controlled sequence shift intervention we use to evaluate sensitivity to positional misalignment in MDLMs. We first identify positions within text spans that are already unmasked, defined as token indices whose

immediate left and right neighbors are also unmasked. We then uniformly sample K *shift boundary* locations, then locate the contiguous block of unmasked tokens immediately to their right and rotate this block by one position, moving a $\langle \text{MASK} \rangle$ token into the span and shifting the text tokens right by one index (see the example below):

Intervention Example

Before:	...	A	B	C	D	$\langle \text{MASK} \rangle$...
After:	...	A	$\langle \text{MASK} \rangle$	B	C	D	...

This operation preserves sequence length and token identities, and does not overwrite or delete tokens. Since all *shift boundaries* are determined from the same sequence snapshot and correspond to distinct boundaries, the shifted spans do not overlap.

Interventions are applied at fixed early decoding steps, every 0.05 diffusion time units for $t \geq 0.5$, yielding 10 intervention steps per generation. At each scheduled step, K *shift boundaries* are selected and shifted simultaneously. Thus, a total of $10 \times K$ one-index shift operations are introduced over the decoding process. While each individual operation introduces only a local one-index positional shift, repeating such interventions during early decoding allows these small misalignments to accumulate under irreversible generation.

3.2. Experimental Setup

Models and generation configuration. Experiments are conducted using LLaDA-8B-Instruct (Nie et al., 2025b) and LLaDA-1.5 (Zhu et al., 2025), two widely used MDLM variants that differ in their post-training objectives and training data. Unless otherwise stated, we adopt a fixed inference configuration across all experiments, including response length $L = 1024$, $N = 512$ diffusion steps, and the standard low-confidence remasking strategy used in LLaDA. This setup ensures that observed differences are attributable to the applied interventions rather than decoding hyperparameters.

Benchmark and evaluation. Evaluation is performed on a balanced subset of Arena-Hard-v2.0 (Li et al., 2025b; 2024), consisting of 98 examples. We follow the official Arena-Hard evaluation protocol and report win rates separately on the hard-prompt and creative-writing subsets. Since the goal is to measure relative degradation caused by positional perturbations rather than absolute model quality, outputs from the same model generated without intervention are used as the reference baseline, this comparison isolates the effect of accumulated positional misalignment rather than absolute model quality. GPT-4.1 is used as the judge

²Appendix A provides further explanation of shift-like artifacts.

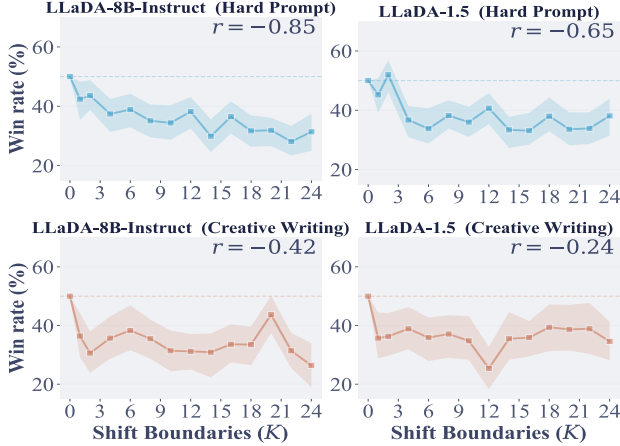


Figure 2. Win rate (%) on Arena-hard as a function of the number of shift boundaries K for LLaDA-8B-Instruct and LLaDA-1.5. Error bands indicate 95% confidence intervals. Win rates are computed against the $K = 0$ (no-intervention) outputs of the same model as the reference, yielding a 50% win-rate baseline (dashed line). The Pearson correlation coefficient r is between K and the win rate; larger r indicates greater sensitivity to the intervention.

model with deterministic decoding³.

3.3. Results

Results are shown in Figure 2, where r indicates the Pearson correlation coefficient between K and the win rate. Across both models, namely LLaDA-8B-Instruct and LLaDA-1.5, generation quality degrades consistently as the number of *shift boundaries* K increases. The results show that repeated one-index positional shifts lead to substantial degradation in generation quality. These findings motivate the alignment-flexible training approach introduced in Section 4.

4. Relaxing Positional Alignment

The standard training objective for MDLMs uses a masked cross-entropy loss, as defined in Eq. (2). This objective supervises each masked position independently and thus assumes a fixed one-to-one correspondence between output positions and target tokens. Consequently, training enforces a strict positional alignment.

To relax this constraint, we introduce a special `<SLACK>` token that can absorb local positional mismatch. We implement this using CTC, which allows the model to predict a longer latent sequence that may include `<SLACK>` tokens and repeated tokens. The CTC collapse operation maps this latent sequence to the target by removing `<SLACK>` tokens and merging adjacent duplicates; as a result, supervision is no longer applied at fixed output positions. Although

³We choose GPT-4.1 for reproducibility since GPT-5 does not support deterministic decoding.

CTC was originally developed for speech recognition, the same mechanism directly applies when the correspondence between prediction positions and target tokens is uncertain.

4.1. CTC-Based Objective

We start from the gold target response $r_0 \in \mathcal{V}^L$, insert `<SLACK>` tokens to obtain a slack-augmented target $\tilde{r}_0 \in (\mathcal{V} \cup \{<SLACK>\})^{\tilde{L}}$, where \tilde{L} is the alignment length including `<SLACK>` tokens, and apply masking as in standard MDLM training. Specifically, given a mask ratio sampled as $t \sim \mathcal{U}[0, 1]$, we construct a corrupted response sequence \tilde{r}_t by replacing a subset of tokens in \tilde{r}_0 with `<MASK>`, paired with a prompt q_0 . Let $a = (a^1, \dots, a^{\tilde{L}})$ be a latent alignment sequence, where $a_i \in \mathcal{V} \cup \{<SLACK>\}$. Under the standard CTC conditional independence assumption, the alignment probability factorizes as:

$$P^{\text{CTC}}(a \mid q_0, \tilde{r}_t) = \prod_{i=1}^{\tilde{L}} P_{\theta}(a^i \mid q_0, \tilde{r}_t). \quad (4)$$

The CTC likelihood of the clean target response r_0 is obtained by marginalizing over all alignment sequences that collapse to r_0 :

$$P^{\text{CTC}}(r_0 \mid q_0, \tilde{r}_t) = \sum_{a \in \beta^{-1}(r_0)} P^{\text{CTC}}(a \mid q_0, \tilde{r}_t), \quad (5)$$

where $\beta^{-1}(r_0)$ returns all possible alignments compatible with r_0 by collapses consecutive repetitions in a (i.e., replaces each maximal run of identical symbols with a single symbol), and then removes all `<SLACK>` symbols. Then the corresponding CTC training objective is written as follows:

$$\mathcal{L}_{\theta, t}^{\text{CTC}} = -\mathbb{E}_{t, q_0, r_0, \tilde{r}_t} [\log P^{\text{CTC}}(r_0 \mid q_0, \tilde{r}_t)]. \quad (6)$$

4.2. Combined Objective

We redefine the SFT objective to incorporate the CTC objective into SFT as follows:

$$\mathcal{L}_{\theta, t}^{\text{SFT}} = \mathcal{L}_{\theta, t}^{\text{CE}} + \lambda \mathcal{L}_{\theta, t}^{\text{CTC}}, \quad (7)$$

where λ controls the contribution of the CTC term. The CTC term is computed against the original slack-free target r_0 , as explained in Eq. (6), whereas the CE term is computed over the slack-augmented target \tilde{r}_0 . Moreover, both CTC and CE terms use the corrupted response sequence \tilde{r}_t , which is derived from \tilde{r}_0 . Therefore, when computing the CE term, we compute Eq. (2) by substituting r_t and r_0 with \tilde{r}_t and \tilde{r}_0 , respectively.

This encourages the model to emit `<SLACK>` tokens in \tilde{L} predictions when needed to accommodate positional uncertainty, while keeping the supervised output content equal to r_0 after collapse.

Table 1. Performance comparison on open-ended text generation benchmarks. The CTC-trained model is obtained by applying the combined CTC and cross-entropy objective to LLaDA-8B-Instruct, while the CE-only baseline is trained with the cross-entropy objective under identical settings. Results for LLaDA-1.5 are reported for reference. Blue cells indicate cases where the CTC-trained model outperforms both LLaDA-8B-Instruct and the CE-only Baseline, and bold numbers denote the best result for each benchmark. Arena-Hard scores are pairwise win rates against LLaDA-8B-Instruct; 95% bootstrap confidence intervals are computed using the official evaluation protocol.

	CTC + CE	CE Only	LLaDA-8B-Instruct	LLaDA-1.5
Arena-hard* (Hard-Prompt)	51.4 (−2.3/ + 2.0)	27.2 (−2.2/ + 1.8)	50.0 (−0.0/ + 0.0)	58.5 (−2.5/ + 2.0)
Arena-hard* (Creative-Writing)	80.2 (−2.3/ + 1.9)	31.4 (−3.0/ + 2.4)	50.0 (−0.0/ + 0.0)	66.0 (−2.3/ + 2.3)
Creative-Writing-Bench v3	27.4	25.7	24.1	24.9
MTBench	3.7	2.2	2.8	3.3
WildBench	−1.7	−4.5	−3.3	−2.5

4.3. Train–Inference Consistent Denoising

With the introduction of the CTC objective, adjacent identical tokens are treated as equivalent to a single token under the CTC collapse operation, together with `<SLACK>` tokens. This equivalence allows the model to generate the same token at multiple adjacent positions.

During training, intermediate noisy states are constructed by inserting `<SLACK>` tokens and applying random masking, and therefore contain no repeated tokens. At inference time, however, the CTC formulation permits repeated tokens in intermediate denoising states, creating a mismatch between training and inference.

To address this issue, we explicitly handle CTC-induced repetitions during decoding. Specifically, at the end of each denoising step, after token transfer and confidence-based remasking, we identify adjacent positions whose decoded tokens are identical, excluding masked positions and `<SLACK>` tokens. For each adjacent duplicate pair, the later position is converted into a `<SLACK>` token. This greedy and local operation preserves the fixed sequence length while ensuring that intermediate denoising states remain consistent with the alignment flexibility induced by the CTC training objective.

5. Experiments

To demonstrate the effectiveness of our method, we conduct experiments on five open-ended generation benchmarks⁴.

5.1. Data Preparation

For each training example, we augment the target response with a variable number of `<SLACK>` tokens to introduce alignment flexibility. The total amount of slack is controlled by a per-example slack ratio, which is sampled uniformly at

⁴We describe the further implementation details, including training framework, training hyperparameters, λ for CTC term in training, and benchmark implementation in Appendix B

random and capped at a fixed maximum.

Concretely, we sample a slack ratio $s \sim \mathcal{U}[0, s_{\max}]$, where $s_{\max} = 0.5$ in all experiments. Given a clean response of length L , this ratio determines the number of `<SLACK>` tokens as $\lfloor s \cdot L \rfloor$. These tokens are inserted at random positions within the response, increasing its effective length. The inserted `<SLACK>` tokens serve as alignment buffers that allow the model to absorb local positional uncertainty without committing to a specific token placement.

In addition to explicit insertion, `<SLACK>` tokens may also be obtained by repurposing padding positions. As noted in prior LLaDA work, during SFT, sequences within each mini-batch are padded to a uniform length by appending end-of-sequence tokens (`<EOS>`) to shorter responses, and these padding `<EOS>` tokens are supervised. While this teaches the model to control response length by explicitly generating `<EOS>`, it also increases the amount of supervision placed on `<EOS>` tokens.

To reduce this effect, we allow a portion of the padding budget to be converted into `<SLACK>` tokens. Specifically, after determining the total number of slack tokens for a response, if unused sequence capacity remains, we replace a subset of the padding `<EOS>` tokens with `<SLACK>` and randomly place them within the sequence, subject to the fixed length constraint. The number of such conversions is controlled by a separate ratio and capped at a fixed fraction of the response length. In practice, this reassigns part of the padding capacity to `<SLACK>` tokens while leaving the supervision on the final `<EOS>` unchanged.

5.2. Experimental Setup

Models. We evaluate LLaDA-8B-Instruct (Nie et al., 2025b), an open MDLM trained with supervised fine-tuning, and LLaDA-1.5 (Zhu et al., 2025), a reinforcement learning variant of LLaDA-8B-Instruct, which was trained on an extra 350K preference pairs and serves as a strong external reference for generation quality. In addition, we train a

model with a combined CTC and cross-entropy objective as the CTC-trained model, and a model trained with the same architecture, initialization, data, and optimization settings but only with a standard cross-entropy objective as the CE-only baseline.

Benchmarks. We evaluate open-ended generation quality on five benchmarks: Arena-Hard-v2.0 (Li et al., 2025b; 2024) (including hard-prompt and creative-writing categories, we report both), MTBench (Zheng et al., 2023), WildBench (Lin et al., 2025), Writing Bench (Wu et al., 2025a), and Creative Writing v3 (Paech, 2025). Note that for Arena-Hard-v2.0, it uses pairwise win rates against a CE-only baseline. We replace the standard o3 baseline with LLaDA-8B-Instruct, as o3 produces near-degenerate outcomes for MDLMs. Results are intended for controlled within-family comparison in this work and are not leaderboard-comparable.

SFT setup. We used the official filtered Magpie dataset (Xu et al., 2025), which contains approximately 300k high-quality instruction-following examples synthesized from Llama-3-70B-Instruct (Grattafiori et al., 2024). To balance computational cost and the effect of the CTC objective, we further filter the dataset by response length, retaining examples with responses between 512 and 1024 tokens under the LLaDA tokenizer. This results in 291k training samples. Both the CTC-trained model and the CE-only baseline are trained on this dataset for three epochs using LoRA (Hu et al., 2022) adapters, corresponding to a total of 35,955 training steps.

Inference setup. Diffusion-based text generation is sensitive to inference-time hyperparameters, such as sequence length, denoising schedule, and masking strategy. Since our goal is to compare training objectives rather than to optimize decoding, we fix the inference configuration across all models to enable controlled and comparable evaluation: sequence length $L = 1024$, $N = 512$ diffusion steps, and the standard low-confidence remasking strategy used in LLaDA.

5.3. Results

Table 1 reports results on all target benchmarks. Blue cells indicate cases where the CTC-trained model outperforms both the CE-only baseline and LLaDA-8B-Instruct, while bold numbers denote the best result within each row⁵.

Consistent gains over the matched baseline. Across all evaluated benchmarks, the CTC-trained model outperforms the CE-only baseline, which is trained under identical settings but without the CTC objective. Since both models

⁵See Appendix C for further experiments on model’s broader capability for CTC-trained model.

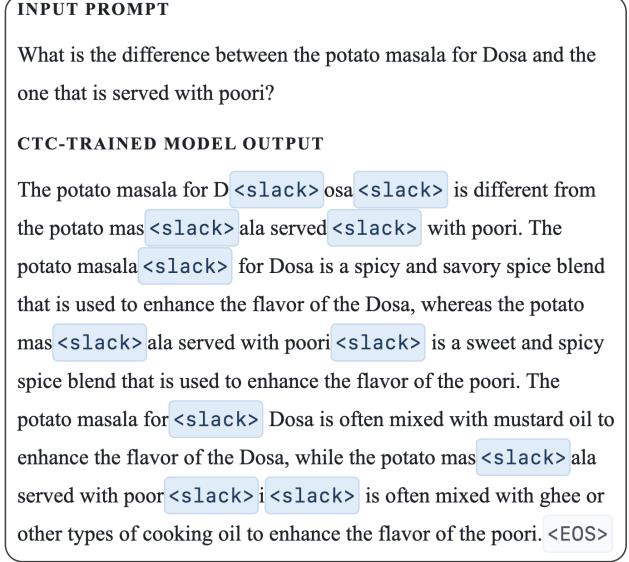


Figure 3. Illustration of <SLACK> token placement in the CTC-trained model. <SLACK> is observed both within tokenized words ((e.g., D<SLACK>osa, mas<SLACK>ala)) and between words, where it functions as mid-text padding. This suggests <SLACK> can act as a flexible buffer at different locations in the sequence.

share the same architecture, initialization, data, and training schedule, this comparison isolates the effect of the training objective. Our results suggest that relaxing strict positional supervision in MDLM is effective in improving open-ended generation quality even under the basic choice of CTC.

Effect of standard MDLM SFT. The CE-only baseline, trained with the standard MDLM SFT objective, underperforms LLaDA-8B-Instruct on four out of five benchmarks. While differences in instruction-tuning data and training pipelines are likely contributors, this gap highlights the sensitivity of diffusion-based LMs to training objectives and alignment assumptions in the instruction-tuning regime.

Comparison with LLaDA-1.5. The CTC-trained model exceeds LLaDA-1.5 on the Creative-Writing subset of Arena-Hard-v2.0 as well as on Creative-Writing-Bench v3, MTBench, and WildBench. LLaDA-1.5 is trained with reinforcement learning on a $1.2 \times$ larger closed dataset, whereas our model is trained with SFT on an open dataset. Despite these differences, the CTC-trained model achieves competitive or superior performance on several benchmarks. Taken together, these results suggest that positional alignment is a factor affecting the effectiveness of standard training objectives for MDLMs, with particularly pronounced gains on open-ended and creative generation tasks.

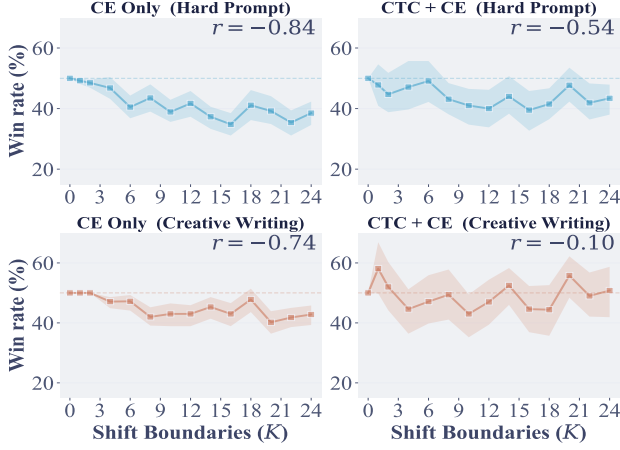


Figure 4. Win rate (%) on Arena-hard as a function of the number of shift boundaries K for the CTC-trained model and the CE-only baseline. Error bands indicate 95% confidence intervals. Win rates are computed against the $K = 0$ (no-intervention) outputs of the same model as the reference, yielding a 50% win-rate baseline (dashed line). The Pearson correlation coefficient r is between K and the win rate; r indicates weaker sensitivity to the intervention.

5.4. Discussions

CTC improves robustness to token misalignment. To evaluate whether the CTC objective improves robustness to token position misalignment, we repeat the experiment from Section 3 for both the CTC-trained model and the CE-only baseline. Figure 4 summarizes the results. The CE-only baseline exhibits the same sensitivity to positional misalignment observed for LLaDA-8B-Instruct and LLaDA-1.5 in Figure 2: the relative win rate drops substantially under intervention, and stronger interventions lead to larger declines. In contrast, the CTC-trained model is more stable, as it can absorb small positional shifts by assigning misaligned positions to the <SLACK> token. Quantitatively, the Pearson correlation coefficient r between win rate and intervention strength is -0.85 for LLaDA-8B-Instruct and -0.54 for the CTC-trained model in the hard-prompt category. For the creative writing category, the corresponding values are -0.42 for LLaDA-8B-Instruct and -0.10 for the CTC-trained model.

The <SLACK> token behavior. Figure 3 shows how the CTC-trained model uses the <SLACK> token during generation. We observe <SLACK> appearing both within subword sequences (e.g., D<SLACK>osa) and as standalone tokens between words. In the latter case, it often serves as mid-text padding to adjust the effective sequence length. We also observe substantial variation in how frequently <SLACK> is used across different generations: some outputs contain many <SLACK> tokens, while others contain few or none. Together, these patterns indicate that <SLACK> provides alignment flexibility at multiple granularities, ranging from

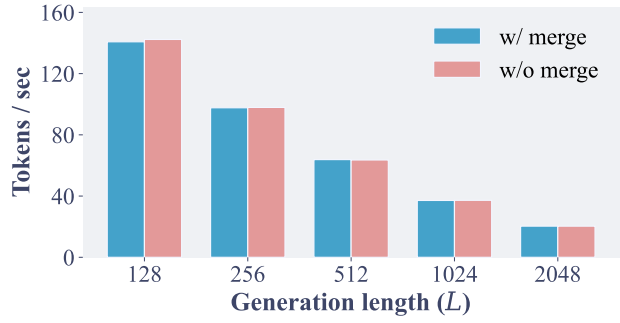


Figure 5. Tokens per second for the CTC-trained model with and without the merge operation during decoding.

subword-level spans to word-boundary positions.

Generation overhead of CTC decoding. To test whether the merge operation used in CTC decoding adds computational overhead, we measure generation throughput with and without merge across a range of generation lengths L . For each L , we set the number of diffusion steps to $N = L/2$ and compute throughput as tokens per second using the reported generation time. For each configuration, we perform 6 warm-up generations (excluded from measurement), followed by 30 timed runs. Figure 5 shows that generation throughput remains essentially unchanged when merge is enabled, indicating that the merge operation does not introduce a meaningful slowdown in this setting.

6. Related Work

6.1. Positional Misalignment

A line of work addresses failures caused by fixed-length canvases and rigid position-wise structure in diffusion-based (and related) text generation, especially when the desired output length or span boundaries are uncertain (Zhang et al., 2025a; Wu et al., 2025b; Yang et al., 2025; Kim et al., 2025a; Havasi et al., 2025; Li et al., 2025a). These approaches improve robustness by enabling variable-length generation via mechanisms such as token position adjustment, end-of-sequence prediction, or explicit insertion and deletion operations. DreamOn (Wu et al., 2025b) is most closely related in motivation, as it also introduces auxiliary tokens during generation. However, DreamOn is designed for code infilling and uses special state tokens to dynamically expand or contract the masked canvas, thereby adapting the generation target to the task’s span-length requirements.

In contrast, our work studies token misalignment that arises under standard open-ended generation. Rather than modifying the target sequence or adjusting the effective canvas, we introduce a <SLACK> token to absorb alignment uncertainty during decoding. This allows the model to remain within the MDLM generation setup while improving robust-

ness in position-sensitive, open-ended generation tasks.

6.2. Early Commitment / Token-level Self-correction

Several recent works study the early commitment or absorbing state issue in MDLMs, where errors introduced early in decoding can persist and cascade through subsequent steps (Wang et al., 2025; Lee et al., 2025; Peng et al., 2025). Much of this literature focuses on enabling token identity revision, either by allowing explicit re-masking or refinement during inference (Wang et al., 2025; Peng et al., 2025) or by improving inference-time unmasking decisions and parallel decoding strategies (Lee et al., 2025; Horvitz et al., 2025; Jazbec et al., 2025). Another line of work introduces pre-training or fine-tuning objectives that support self-correction via token-quality estimation and targeted refinement (Huang et al., 2025; Kim et al., 2025b; Zhang et al., 2025b).

Our work focuses on positional sensitivity: we treat early committed tokens as immutable and analyze how index-level misalignment propagates through subsequent generation, leading to systematic degradation.

6.3. Block Diffusion Sampling

Block diffusion (Arriola et al., 2025) refers to the generation strategies that update groups of token positions jointly during diffusion-based generation. Several MDLMs support block diffusion purely as an inference-time decoding choice, without modifying the forward noising process or training objective (Nie et al., 2025b; Zhu et al., 2025; Ye et al., 2025). In these models, block diffusion groups token positions during the reverse process while retaining the one-to-one positional supervision used during training.

Our work operates under the same MDLM architecture and decoding setup and is orthogonal to, and can be combined with, block-based decoding.

6.4. Flexible Alignment Training Objective.

A range of alignment-flexible training objectives have been explored to relax strict position-wise supervision by marginalizing over latent alignments or edit paths (Ristad & Yianilos, 1998; Oncina & Sebban, 2006; Cuturi & Blondel, 2017; Sarawagi & Cohen, 2004). CTC is a representative instance of this class, originally introduced for sequence prediction problems with uncertain alignment, most notably in speech recognition (Graves et al., 2006; Graves, 2012; Graves et al., 2013; Higuchi et al., 2020). Variants and applications of CTC have since been studied beyond speech (Libovický & Helcl, 2018; Saharia et al., 2020; Xu et al., 2023; Fujita et al., 2024).

In this work, we adopt CTC as a simple and well-established representative of alignment-flexible objectives. Our focus is

not on CTC itself, but on the broader principle of relaxing strict positional supervision during training to better match the irreversible decoding dynamics of MDLMs.

7. Limitations

We instantiate the standard CTC objective as a flexible alignment objective, which induces a collapse operation that removes both `<SLACK>` tokens and repeated adjacent tokens. This merging behavior can be undesirable for tasks that require exact surface forms, such as numeric strings or formatting symbols. As a result, it may introduce failure modes on format-sensitive evaluations; see Appendix C for detailed examples. Since CTC represents a basic form of flexible alignment, a natural next step is to explore more advanced or task-specific alignment objectives within MDLMs, which may provide a more robust solution to positional misalignment while avoiding these surface-form issues.

Our experiments are limited to the SFT of a standard MDLM. The effect of relaxing positional alignment during pre-training remains unexplored. Integrating flexible alignment objectives directly into the pre-training stage is a natural direction for future work and may lead to MDLMs that natively support alignment flexibility. Finally, we do not investigate architectural-level integration of flexible alignment mechanisms. Such integration could further improve robustness to token misalignment and may yield additional gains beyond objective-level modifications.

8. Conclusion

This work identifies strict position-level supervision as a factor in degraded open-ended generation in MDLMs. Due to the irreversible nature of standard MDLM decoding, small token misalignments can persist and cascade, leading to substantial degradation in generation quality. We demonstrate this effect using a controlled intervention experiment and show that repeated one-position shifts can affect open-ended generation performance. These results indicate that strict one-to-one positional alignment is misaligned with the decoding dynamics of MDLMs.

Based on this diagnosis, we introduce a minimal relaxation of positional supervision using CTC, a simple and well-studied alignment-flexible objective, to introduce a special `<SLACK>` token to absorb positional misalignment. When applied during SFT, this approach improves robustness to positional errors and consistently outperforms on five open-ended generation benchmarks on LLaDA-8B-Instruct.

Overall, our results show that relaxing positional alignment improves open-ended generation in MDLMs. These findings identify strict positional supervision as an important factor affecting failures and indicate that introducing align-

ment flexibility is an effective way to mitigate this issue, making it a promising direction for further study.

Acknowledgment

Author Contributions. All authors contributed to early discussions that shaped the research direction. M. Ye led the implementation of training data preparation, the training pipeline, and the benchmarking pipeline. R. Takahashi led the early-stage supervised fine-tuning implementation supporting the proof of concept and implemented the local evaluation server. K. Kudo and J. Suzuki contributed through intensive technical discussions that refined the problem formulation and guided the project direction. M. Ye drafted the initial manuscript, R. Takahashi wrote the initial version of Section 2, and took primary responsibility for collecting, verifying, and maintaining the citations. K. Kudo produced all figures, and J. Suzuki provided detailed feedback on the mathematical formulations and manuscript.

Acknowledgments. We want to express our gratitude to the members of the Tohoku NLP Group for their insightful comments. We used ABCI 3.0 provided by AIST and AIST Solutions with support from “ABCI 3.0 Development Acceleration Use” for our main experiments. A part of the computation was carried out using the computer resource offered under the category of General Projects by Research Institute for Information Technology, Kyushu University. This work was supported by the “R&D Hub Aimed at Ensuring Transparency and Reliability of Generative AI Models” project of the Ministry of Education, Culture, Sports, Science and Technology; JST Moonshot R&D Grant Number JPMJMS2011-35 (fundamental research); JSPS KAKENHI Grant Numbers JP25KJ0615; JST BOOST, Japan Grant Number JPMJBS2421.

Impact Statement

This paper presents work whose goal is to advance the understanding of MDLMs. We study a training-time objective modification and evaluate its effect on generation quality under controlled experimental settings. We do not conduct a dedicated analysis of social biases, toxicity, or other downstream harms in model outputs. The models produced in this work are not intended for deployment or public use beyond reproducing the reported experiments. As this work focuses on model diagnostics and training objectives rather than new capabilities or deployment scenarios, we do not identify specific societal or ethical impacts that require separate discussion beyond those commonly associated with research on language models.

References

Arriola, M., Sahoo, S. S., Gokaslan, A., Yang, Z., Qi, Z., Han, J., Chiu, J. T., and Kuleshov, V. Block diffusion: Interpolating between autoregressive and diffusion language models. In *The Thirteenth International Conference on Learning Representations*, 2025. URL <https://openreview.net/forum?id=tyEyYT267x>.

Austin, J., Odena, A., Nye, M., Bosma, M., Michalewski, H., Dohan, D., Jiang, E., Cai, C., Terry, M., Le, Q., and Sutton, C. Program synthesis with large language models, 2021. URL <https://arxiv.org/abs/2108.07732>.

Brown, T. B., Mann, B., Ryder, N., Subbiah, M., Kaplan, J., Dhariwal, P., Neelakantan, A., Shyam, P., Sastry, G., Askell, A., Agarwal, S., Herbert-Voss, A., Krueger, G., Henighan, T., Child, R., Ramesh, A., Ziegler, D. M., Wu, J., Winter, C., et al. Language models are few-shot learners. In *The Thirty-fourth Annual Conference on Neural Information Processing Systems*, 2020. URL https://proceedings.neurips.cc/paper_files/paper/2020/file/1457c0d6bfcb4967418bfb8ac142f64a-Paper.pdf.

Chang, H., Zhang, H., Jiang, L., Liu, C., and Freeman, W. T. Maskgit: Masked generative image transformer. *arXiv preprint arXiv:2202.04200*, 2022. URL <https://arxiv.org/abs/2202.04200>.

Cobbe, K., Kosaraju, V., Bavarian, M., Chen, M., Jun, H., Kaiser, L., Plappert, M., Tworek, J., Hilton, J., Nakano, R., Hesse, C., and Schulman, J. Training verifiers to solve math word problems. *arXiv preprint arXiv:2110.14168*, 2021. URL <https://arxiv.org/abs/2110.14168>.

Cuturi, M. and Blondel, M. Soft-dtw: a differentiable loss function for time-series. In *Proceedings of the 34th International Conference on Machine Learning - Volume 70*, ICML’17, pp. 894–903. JMLR.org, 2017.

Fujita, Y., Watanabe, S., Chang, X., and Maekaku, T. Lv-ctc: Non-autoregressive asr with ctc and latent variable models. *arXiv preprint arXiv:2403.19207*, 2024. URL <https://arxiv.org/abs/2403.19207>.

Grattafiori, A., Dubey, A., Jauhri, A., Pandey, A., Kadian, A., Al-Dahle, A., Letman, A., Mathur, A., Schelten, A., Vaughan, A., Yang, A., Fan, A., Goyal, A., Hartshorn, A., Yang, A., Mitra, A., Sravankumar, A., Korenev, A., Hinsvark, A., et al. The llama 3 herd of models, 2024. URL <https://arxiv.org/abs/2407.21783>.

Graves, A. Sequence transduction with recurrent neural networks. *arXiv preprint arXiv:1211.3711*, 2012. URL <https://arxiv.org/abs/1211.3711>.

Graves, A., Fernández, S., Gomez, F., and Schmidhuber, J. Connectionist temporal classification: labelling unsegmented sequence data with recurrent neural networks. In *Proceedings of the 23rd International Conference on Machine Learning*, ICML '06, pp. 369–376, New York, NY, USA, 2006. Association for Computing Machinery. ISBN 1595933832. doi: 10.1145/1143844.1143891. URL <https://doi.org/10.1145/1143844.1143891>.

Graves, A., rahman Mohamed, A., and Hinton, G. Speech recognition with deep recurrent neural networks. *arXiv preprint arXiv:1303.5778*, 2013. URL <https://arxiv.org/abs/1303.5778>.

Havasi, M., Karrer, B., Gat, I., and Chen, R. T. Q. Edit flows: Flow matching with edit operations. *arXiv preprint arXiv:2506.09018*, 2025. URL <https://arxiv.org/abs/2506.09018>.

Hendrycks, D., Burns, C., Basart, S., Critch, A., Li, J., Song, D., and Steinhardt, J. Aligning {ai} with shared human values. In *International Conference on Learning Representations*, 2021a. URL https://openreview.net/forum?id=dNy_RKzJacY.

Hendrycks, D., Burns, C., Basart, S., Zou, A., Mazeika, M., Song, D., and Steinhardt, J. Measuring massive multitask language understanding. In *The Ninth International Conference on Learning Representations*, 2021b. URL <https://openreview.net/forum?id=d7KBjmI3GmQ>.

Higuchi, Y., Watanabe, S., Chen, N., Ogawa, T., and Kobayashi, T. Mask etc: Non-autoregressive end-to-end asr with etc and mask predict. *arXiv preprint arXiv:2005.08700*, 2020. URL <https://arxiv.org/abs/2005.08700>.

Horvitz, Z., Singhal, R., Zou, H., Domingo-Enrich, C., Yu, Z., Ranganath, R., and McKeown, K. No compute left behind: Rethinking reasoning and sampling with masked diffusion models. *arXiv preprint arXiv:2510.19990*, 2025. URL <https://arxiv.org/abs/2510.19990>.

Hu, E. J., yelong shen, Wallis, P., Allen-Zhu, Z., Li, Y., Wang, S., Wang, L., and Chen, W. LORA: Low-rank adaptation of large language models. In *International Conference on Learning Representations*, 2022. URL <https://openreview.net/forum?id=nZeVKeeFYf9>.

Huang, Z., Wang, Y., Chen, Z., and Qi, G.-J. Don't settle too early: Self-reflective remasking for diffusion language models. *arXiv preprint arXiv:2509.23653*, 2025. URL <https://arxiv.org/abs/2509.23653>.

Jazbec, M., Olausson, T. X., Béthune, L., Ablin, P., Kirchhof, M., Monteiro, J., Turrisi, V., Ramapuram, J., and Cuturi, M. Learning unmasking policies for diffusion language models. *arXiv preprint arXiv:2512.09106*, 2025. URL <https://arxiv.org/abs/2512.09106>.

Kim, J., Cheuk-Kit, L., Domingo-Enrich, C., Du, Y., Kakade, S., Nogotiaoco, T., Chen, S., and Albergo, M. Any-order flexible length masked diffusion. *arXiv preprint arXiv:2509.01025*, 2025a. URL <https://arxiv.org/abs/2509.01025>.

Kim, J., Kim, S., Lee, T., Pan, D. Z., Kim, H., Kakade, S., and Chen, S. Fine-tuning masked diffusion for provable self-correction. *arXiv preprint arXiv:2510.01384*, 2025b. URL <https://arxiv.org/abs/2510.01384>.

Lee, S., Kim, S., Park, J., and Park, D. Lookahead unmasking elicits accurate decoding in diffusion language models. *arXiv preprint arXiv:2511.05563*, 2025. URL <https://arxiv.org/abs/2511.05563>.

Li, J., Dong, X., Zang, Y., Cao, Y., Wang, J., and Lin, D. Beyond fixed: Variable-length denoising for diffusion large language models. *arXiv preprint arXiv:2508.00819*, 2025a. URL <https://arxiv.org/abs/2508.00819>.

Li, T., Chiang, W.-L., Frick, E., Dunlap, L., Zhu, B., Gonzalez, J. E., and Stoica, I. From live data to high-quality benchmarks: The arena-hard pipeline, April 2024. URL <https://lmsys.org/blog/2024-04-19-arena-hard/>.

Li, T., Chiang, W.-L., Frick, E., Dunlap, L., Wu, T., Zhu, B., Gonzalez, J. E., and Stoica, I. From crowdsourced data to high-quality benchmarks: Arena-hard and benchmark builder pipeline. In *Forty-second International Conference on Machine Learning*, 2025b. URL <https://openreview.net/forum?id=KfTf9vFvSn>.

Libovický, J. and Helcl, J. End-to-end non-autoregressive neural machine translation with connectionist temporal classification. In Riloff, E., Chiang, D., Hockenmaier, J., and Tsujii, J. (eds.), *Proceedings of the 2018 Conference on Empirical Methods in Natural Language Processing*, pp. 3016–3021, Brussels, Belgium, October–November 2018. Association for Computational Linguistics. doi: 10.18653/v1/D18-1336. URL <https://aclanthology.org/D18-1336/>.

Lin, B. Y., Deng, Y., Chandu, K., Ravichander, A., Pyatkin, V., Dziri, N., Bras, R. L., and Choi, Y. Wildbench: Benchmarking LLMs with challenging tasks from real

users in the wild. In *The Thirteenth International Conference on Learning Representations*, 2025. URL <https://openreview.net/forum?id=MKEHCx25xp>.

Loshchilov, I. and Hutter, F. Decoupled weight decay regularization. In *International Conference on Learning Representations*, 2019. URL <https://openreview.net/forum?id=Bkg6RiCqY7>.

Nie, S., Zhu, F., Du, C., Pang, T., Liu, Q., Zeng, G., Lin, M., and Li, C. Scaling up masked diffusion models on text. In *The Thirteenth International Conference on Learning Representations*, 2025a. URL <https://openreview.net/forum?id=WNvvwK0tut>.

Nie, S., Zhu, F., You, Z., Zhang, X., Ou, J., Hu, J., Zhou, J., Lin, Y., Wen, J.-R., and Li, C. Large language diffusion models. *arXiv preprint arXiv:2502.09992*, 2025b. URL <https://arxiv.org/abs/2502.09992>.

Oncina, J. and Sebban, M. Learning stochastic edit distance: Application in handwritten character recognition. *Pattern Recognition*, 39(9):1575–1587, 2006. ISSN 0031-3203. doi: <https://doi.org/10.1016/j.patcog.2006.03.011>. URL <https://www.sciencedirect.com/science/article/pii/S0031320306001245>.

Paech, S. J. Eq-bench creative writing benchmark v3. <https://github.com/EQ-bench/creative-writing-bench>, 2025.

Peng, F. Z., Bezemek, Z., Patel, S., Rector-Brooks, J., Yao, S., Bose, A. J., Tong, A., and Chatterjee, P. Path planning for masked diffusion model sampling. *arXiv preprint arXiv:2502.03540*, 2025. URL <https://arxiv.org/abs/2502.03540>.

Rein, D., Hou, B. L., Stickland, A. C., Petty, J., Pang, R. Y., Dirani, J., Michael, J., and Bowman, S. R. GPQA: A graduate-level google-proof q&a benchmark. In *First Conference on Language Modeling*, 2024. URL <https://openreview.net/forum?id=Ti67584b98>.

Ristad, E. and Yianilos, P. Learning string-edit distance. *IEEE Transactions on Pattern Analysis and Machine Intelligence*, 20(5):522–532, 1998. doi: 10.1109/34.682181.

Saharia, C., Chan, W., Saxena, S., and Norouzi, M. Non-autoregressive machine translation with latent alignments. In Webber, B., Cohn, T., He, Y., and Liu, Y. (eds.), *Proceedings of the 2020 Conference on Empirical Methods in Natural Language Processing (EMNLP)*, pp. 1098–1108, Online, November 2020. Association for Computational Linguistics. doi: 10.18653/v1/2020.emnlp-main.83. URL <https://aclanthology.org/2020.emnlp-main.83/>.

Sahoo, S. S., Arriola, M., Gokaslan, A., Marroquin, E. M., Rush, A. M., Schiff, Y., Chiu, J. T., and Kuleshov, V. Simple and effective masked diffusion language models. In *The Thirty-eighth Annual Conference on Neural Information Processing Systems*, 2024. URL <https://openreview.net/forum?id=L4uaAR4ArM>.

Sarawagi, S. and Cohen, W. W. Semi-markov conditional random fields for information extraction. In Saul, L., Weiss, Y., and Bottou, L. (eds.), *Advances in Neural Information Processing Systems*, volume 17. MIT Press, 2004. URL https://proceedings.neurips.cc/paper_files/paper/2004/file/eb06b9db06012a7a4179b8f3cb5384d3-Paper.pdf.

Vaswani, A., Shazeer, N., Parmar, N., Uszkoreit, J., Jones, L., Gomez, A. N., Kaiser, L. u., and Polosukhin, I. Attention is all you need. In *Advances in Neural Information Processing Systems*, 2017. URL https://proceedings.neurips.cc/paper_files/paper/2017/file/3f5ee243547dee91fdb053c1c4a845aa-Paper.pdf.

Wang, G., Schiff, Y., Sahoo, S., and Kuleshov, V. Remasking discrete diffusion models with inference-time scaling. In *The Thirty-ninth Annual Conference on Neural Information Processing Systems*, 2025. URL <https://openreview.net/forum?id=IJryQAOy0p>.

Wu, Y., Mei, J., Yan, M., Li, C., Lai, S., Ren, Y., Zijia, W., Zhang, J., Wu, M., Jin, Q., and Huang, F. Writingbench: A comprehensive benchmark for generative writing. In *The Thirty-ninth Annual Conference on Neural Information Processing Systems Datasets and Benchmarks Track*, 2025a. URL <https://openreview.net/forum?id=Pkskg9drDQ>.

Wu, Z., Zheng, L., Xie, Z., Ye, J., Gao, J., Feng, Y., Li, Z., W., V., Zhou, G., and Kong, L. Dreamon: Diffusion language models for code infilling beyond fixed-size canvas, 2025b. URL <https://hkunlp.github.io/blog/2025/dreamon>.

Xu, C., Liu, X., Liu, X., Sun, Q., Zhang, Y., Yang, M., Dong, Q., Ko, T., Wang, M., Xiao, T., Ma, A., and Zhu, J. CTC-based non-autoregressive speech translation. In Rogers, A., Boyd-Graber, J., and Okazaki, N. (eds.), *Proceedings of the 61st Annual Meeting of the Association for Computational Linguistics (Volume 1: Long Papers)*, pp. 13321–13339, Toronto, Canada, July 2023. Association for Computational Linguistics. doi: 10.18653/v1/2023.acl-long.744. URL [https://aclanthology.org/2023.acl-long.744/](https://aclanthology.org/2023.acl-long.744).

Xu, Z., Jiang, F., Niu, L., Deng, Y., Pooventran, R., Choi, Y., and Lin, B. Y. Magpie: Alignment data synthesis from scratch by prompting aligned LLMs with nothing. In *The Thirteenth International Conference on Learning Representations*, 2025. URL <https://openreview.net/forum?id=Pnk7vMbznK>.

Yang, Y., Wang, C., Wang, S., Wen, Z., Qi, B., Xu, H., and Zhang, L. Diffusion llm with native variable generation lengths: Let [eos] lead the way. *arXiv preprint arXiv:2510.24605*, 2025. URL <https://arxiv.org/abs/2510.24605>.

Ye, J., Xie, Z., Zheng, L., Gao, J., Wu, Z., Jiang, X., Li, Z., and Kong, L. Dream 7b: Diffusion large language models. *arXiv preprint arXiv:2508.15487*, 2025. URL <https://arxiv.org/abs/2508.15487>.

Zhang, A., Sivakumar, A., Tang, C.-W., and Thomas, C. Flexible-length text infilling for discrete diffusion models. In Christodoulopoulos, C., Chakraborty, T., Rose, C., and Peng, V. (eds.), *Proceedings of the 2025 Conference on Empirical Methods in Natural Language Processing*, pp. 31344–31359, Suzhou, China, November 2025a. Association for Computational Linguistics. ISBN 979-8-89176-332-6. doi: 10.18653/v1/2025.emnlp-main.1597. URL [https://aclanthology.org/2025.emnlp-main.1597/](https://aclanthology.org/2025.emnlp-main.1597).

Zhang, S., Peng, F. Z., Zhang, Y., Pan, J., and Chrysos, G. G. Corrective diffusion language models. *arXiv preprint arXiv:2512.15596*, 2025b. URL <https://arxiv.org/abs/2512.15596>.

Zhao, S., Gupta, D., Zheng, Q., and Grover, A. d1: Scaling reasoning in diffusion large language models via reinforcement learning. In *ES-FoMo III: 3rd Workshop on Efficient Systems for Foundation Models*, 2025. URL <https://openreview.net/forum?id=t8oYNHAvM9>.

Zheng, L., Chiang, W.-L., Sheng, Y., Zhuang, S., Wu, Z., Zhuang, Y., Lin, Z., Li, Z., Li, D., Xing, E., Zhang, H., Gonzalez, J. E., and Stoica, I. Judging LLM-as-a-judge with MT-bench and chatbot arena. In *Thirty-seventh Conference on Neural Information Processing Systems Datasets and Benchmarks Track*, 2023. URL <https://openreview.net/forum?id=uccHPGDlao>.

Zhu, F., Wang, R., Nie, S., Zhang, X., Wu, C., Hu, J., ZHOU, J., Chen, J., Lin, Y., Wen, J.-R., and Li, C. LLaDA 1.5: Variance-reduced preference optimization for large language diffusion models. *arXiv preprint arXiv:2505.19223*, 2025. URL <https://arxiv.org/abs/2505.19223>.

A. Shift-like Artifacts in Standard Generation

We observe short-range token inconsistency patterns in targeted diagnostic generations from LLaDA-8B-Instruct (Figure 6, 7 and 8), including both local duplications such as “From From”, “The the”, and “Victoria Victoria”, as well as character-level misalignments consistent with small local shifts. Although these patterns may arise from multiple decoding dynamics, they are qualitatively consistent with small local positional misalignment (e.g., shift-like) events during generation. This observation provides illustrative motivation for our perturbation-based analysis of shift sensitivity in Section 3.

B. Implementation Details

B.1. Overall Framework

We perform SFT using the training code of Zhao et al. (2025). The CE-only baseline is trained with the standard diffusion cross-entropy objective, reusing their implementation with only the dataset and preprocessing replaced.

For the CTC-trained model, we introduce an auxiliary CTC alignment loss on the response segment in addition to the diffusion cross-entropy objective. This requires a CTC-specific preprocessing pipeline. For each example, we separate the prompt prefix from the response span, construct a clean target sequence from the unmasked response tokens, and generate a `<SLACK>`-augmented response input by inserting `<SLACK>` tokens according to a random slack budget. End-of-turn and end-of-sequence tokens remain supervised, while padding positions are handled using `<SLACK>` tokens as described in Section 5.1. The final training objective is a weighted sum of diffusion cross-entropy and CTC loss, with the CTC weight set to 0.1. To prevent `<SLACK>` tokens from dominating token-level learning, the contribution of the `<SLACK>` token in the cross-entropy term is down-weighted by a factor of 0.01.

Although we describe this process as inserting `<SLACK>` tokens, training is performed using fixed-length sequences. In practice, slack tokens occupy positions that would otherwise be padding, thereby increasing the effective sequence length of semantic content without changing the tensor length used for batching. The number of `<SLACK>` tokens is sampled from a bounded random budget on a per-example basis.

B.2. Training Hyperparameters

Both the baseline and CTC-trained models are trained under the same optimization settings. We use LoRA adapters with rank $r = 128$, scaling factor $\alpha = 32$, and dropout 0.05, without bias adaptation. Adapters are applied to the transformer projection layers $\{q_proj, k_proj, v_proj\}$, the token embedding layer (`wte`) and the output projection of the feed-forward block (`ff_out`).

Optimization uses AdamW (Loshchilov & Hutter, 2019) with a learning rate of 2×10^{-4} , weight decay 0.1, and gradient clipping at 1.0, under bfloat16 precision. Training is conducted for three epochs with a per-device batch size of 3, no gradient accumulation, and a maximum sequence length of 2048, resulting in 35,955 update steps. We use a linear learning rate schedule without warmup and fix the random seed to 42. Checkpoints are evaluated and saved every 10% of the training steps, and the checkpoint with the lowest evaluation loss is selected. We do not perform any hyperparameter search in this work, including for the CTC loss weight or the `<SLACK>` token contribution in the cross-entropy term.

B.3. Other Details

Benchmark details. We implement all benchmarks using the official repositories released by their respective authors. To ensure consistent model usage across evaluations, we rely on a locally deployed OpenAI-compatible inference interface. Links to the benchmark repositories and their key evaluation settings are summarized in Table 2.

Inference details. During generation for a model trained with CTC, we fix the final position in the sequence to the `<EOS>` token as a minor decoding choice to define a fixed-length generation canvas. After training with the CTC objective, response length is no longer governed by `<EOS>` emission during generation, and `<EOS>` instead serves as a semantic end-of-sequence marker. Fixing the final position provides a consistent terminal boundary, while alignment and length variability are handled by `<SLACK>` tokens at intermediate positions.

Table 2. Summary of the benchmarks used in our evaluation. For each benchmark, we list the task type, evaluation protocol, and a reference to the official repository used in our implementation.

Benchmark	Link
Arena-Hard-v2.0	https://github.com/lmarena/arena-hard-auto?tab=readme-ov-file
Creative-Writing-Bench v3	https://github.com/EQ-bench/creative-writing-bench?tab=readme-ov-file
MTBench	https://github.com/lm-sys/FastChat/tree/main/fastchat/llm.judge
WildBench	https://github.com/allenai/WildBench?tab=readme-ov-file

Table 3. Performance on general benchmarks using the LLaDA-8B-Instruct official evaluation settings. The CTC-trained model and the matched baseline closely track LLaDA-8B-Instruct on GPQA, MMLU, and MBPP, while GSM8K shows a substantially larger drop for the CTC-trained model.

	CTC+CE	CE Only	LLaDA-8B-Instruct [†]
GPQA	30.8	30.8	32.3
MMLU	64.1	65.1	65.4
MBPP	38.4	36.8	39.6
GSM8K	33.1	67.9	68.8

C. Broader Capability Checks

We additionally report results on benchmarks beyond open-ended generation, including general QA (GPQA (Rein et al., 2024), MMLU (Hendrycks et al., 2021b;a)), coding (MBPP (Austin et al., 2021)), and math (GSM8K (Cobbe et al., 2021)). We used LLaDA’s official opencompass evaluation code. We match the generation and evaluation settings used in LLaDA-8B-Instruct’s official scoreboard to enable direct comparison; details can be found at LLaDA’s official repository: <https://github.com/ML-GSAI/LLaDA/blob/main/EVAL.md>.

Table 3 shows small, mixed differences across tasks, with the exception of GSM8K. The baseline closely tracks LLaDA-8B-Instruct, and the CTC-trained model remains similarly close to the matched baseline, with a slight gain on MBPP.

C.1. Analysis of GSM8K Degradation.

On GSM8K, as shown in Figures 9, 10, and 11, we observe a recurring error pattern where the model does not reproduce an exact number from the prompt at the very start of the chain-of-thought reasoning. This arises because the LLaDA tokenizer represents numeric values as sequences of digit-level tokens (e.g., “100” → “1”, “0”, “0”). In particular, for prompt numbers ending in one or more zeros (e.g., 500, 800), the CTC-trained model sometimes drops a trailing zero (e.g., 500 → 50, 800 → 80) and then continues reasoning and computing based on the shortened value. In these cases, the subsequent calculations are internally consistent; the failure traces back to the initial number mismatch, rather than a breakdown of the arithmetic steps themselves.

At the same time, we also observe cases where the model handles trailing-zero numbers correctly and reaches the correct answer, as shown in Figures 12, 13, and 14. Taken together, these examples suggest that the GSM8K drop is tied to occasional surface-form failures on trailing-zero numbers, not that the model is fundamentally unable to handle them. A natural next step, beyond the scope of this work, is to explore objective variants that reduce this failure mode, for example by modifying the standard CTC objective to merge and remove only <SLACK> tokens.

Overall, these results provide a basic check that CTC-based SFT does not substantially disrupt performance on these general benchmarks.

MODEL OUTPUT (SNIPPET)

To determine the quantity of HVAC Crew in the Library, we need to follow a series of steps based on the given relationships.

...

...

...

6. From $(B = B + C)$, we get $(3 = 3 + 9)$, which is consistent.

7. **From** **From** $(O = (B - B))$, we get $(O = (3 - 3) = 0)$.

8. From $(K = O - C)$, we get $(K = 0 - 9 = -9)$.

9. From $(W = 6)$, we get $(W = 6)$.

...

...

...

MODEL OUTPUT (SNIPPET)

1st Header:

Experience Precision: EBAC CD200 Industrial Dehumidifier - 138 PPD | 664 CFM

...

...

...

2nd Body:

The **the** EBAC CD200 Industrial Dehumidifier is engineered to meet the rigorous demands of industrial and commercial settings. With its stainless steel construction, auto/manual mode selection, electronic controls, and high-capacity PTC heater, this dehumidifier ensures reliable and efficient performance removal. Key features include:

- **Stainless Steel Construction:** Built to withstand harsh industrial conditions.
- **Auto/Manual Mode Selection:** Versatile operation for different needs

...

...

...

MODEL OUTPUT (SNIPPET)

The sun was setting over the horizon, casting a warm glow over the bustling city of London Park

...

...

...

She was a vision of beauty, her dark hair cascading down her back like a waterfall of night, her eyes a piercing shade of emerald. Her dress, a deep shade of crimson, fluttered around her like she was made of silk. She approached **Victoria** **Victoria** with a air of confidence, her presence commanding and

...

...

...

Figure 6. Examples of shift-like local inconsistency artifacts in unperturbed LLaDA-8B-Instruct generations. Across diverse prompts, we observe occasional short-range token inconsistency (highlighted), such as “From From”, “the the”, and “Victoria Victoria”. These artifacts are qualitatively consistent with a small local misalignment (e.g., shift) during generation, motivating our controlled “sequence shift” intervention in Section 3.

INPUT PROMPT

Generate the exact same string:

NoTM UZod Ibfpqibj 1bAxXQV tgBfVqCG Omqxow YywTXS uau FfctctLtTC GyBCfqsKr ZQylbcVwIa bsDDojvBox PdIA FPOrgaL
hEZwiHk wNMA1QR QRhzlyQ kOBVMyxj HmMjqmXZJ WdaXLKmcjh wUccTosmq uCfzgqvm GLe 1EngFFBmVf fldhC1
OGoiYVdTqyMn kjNsFLJ CUrXtR QOFytRHYUgg WBM Vfup Ejy CSWvx Zik cJLXkzNjZYB mtsKOTv xdCCeaMScg JPPNZjS ebefpDJc
KTrPJcniT FthmOxOo zagaSUGVsL0G DTW FNnZXYv zMN xevjB fcX0zPewTSN CRdeP dJcloWiCSWeF skUwTIOGG pZyEsQ mwjilNF
XeSwgTwx reaWgm Iqc fUmT NnIUsH1AhEDU psu fPuDGXY UGY 1TM OMW QuKBvtYYKhCZ hwvrYuiX aMakoD jBuLPd zqu vmFhW
gyzzPoCW HOgMBLZqjGei cimqS LZviwt AvYwi aafhyRSzMmG uFHuwJejZN UBmkLzidI Til jIVMMJHu ITOT PjEzyUG WFaykSwO
XqKcgGC OWpAbK SJcpc bHmCL PNEe aDsF SbjkQFUPbyMz ZrxdHv QBoQ rCwfdnK pjhGqRYS1d s1MKWDNsyticF bhqGhiKYvipw
Pudx IwpQTxO UFm jaaQMMVgoo PrPxX zleVtpif cxVvQTqFwi Fkii Fkj dFmyjVkiMoOX HdZMv0ow LHFb iACCXzpF MnkVBH
0QytLqMcYgAL eBNAXF1w vpw LWvZ PylOzvnP RUCYMGW oVcpMZfI Th mP0XukWuI pQxgJG fEvrKuxfoK jkKRQNCChm PAEXcU
sUyLosh kdwBPhpTjqd UUVid vbpKxs esxLxyo xUxbMijRdCd yHoj cVPB0eQpDE afrSK aUcVOL rJEM GLYaaTEJ gmATBzwJaT1f
ObBYrOwYyir xHPkxrtaeS01 E0hpRLvqq Xs1C x1iFUADeB EpGpSFzJ QSBQUEM cgQwMEh kclIK XNRPw1p fhdTtWPWhfB BZj
cZtXQQEHCUww Sjo IYt OKRAXHnrwnj dPjNoz erIDiCE gfRAIpQ zsFN DNfC isonr A0khnToG ThhGkTeXb UakompAepSm LrHxiXrMz
YoE **ZIJ** **cmbcGZiOikaw** LuEHnk sogjivdj1 JOPGFgsNe IYyfQz SNTxmOhAigs oTdcLExQj ZCwDhQsK wCYiNWTXRRMW
hxmDojayqinR EEUHjucR AIdtZMlfjF vTUMsz PVpbfOWzLmEv sDMms onCEzudWr rkKDlrgnnv01 VUpelcjli sRtwZGJ RgfUkmxRz
VsRSGitXasqd qZDB1p ixhaEMbgWEv hLhgRDvA fkw aRBH wsjc OrybgF rBcuqhfdx AZziFFHNxt QwHLbH cyxE zyPha anUizcnJPKd
GWGmn0KEXcJ yQSwFUrcsTqj FKyl AXpK oPfxXYHDcN nHbmnZsHgvaK cyyRFBmLhPm wHTDvw tHujIp IzbrxJydvpth oetyhRbG

MODEL OUTPUT

NoTM UZod Ibfpqibj 1bAxXQV tgBfVqCG Omqxow YywTXS uau FfctctLtTC GyBCfqsKr ZQylbcVwIa bsDDojvBox PdIA FPOrgaL
hEZwiHk wNMA1QR QRhzlyQ kOBVMyxj HmMjqmXZJ WdaXLKmcjh wUccTosmq uCfzgqvm GLe 1EngFFBmVf fldhC1
OGoiYVdTqyMn kjNsFLJ CUrXtR QOFytRHYUgg WBM Vfup Ejy CSWvx Zik cJLXkzNjZYB mtsKOTv xdCCeaMScg JPPNZjS ebefpDJc
KTrPJcniT FthmOxOo zagaSUGVsL0G DTW FNnZXYv zMN xevjB fcX0zPewTSN CRdeP dJcloWiCSWeF skUwTIOGG pZyEsQ mwjilNF
XeSwgTwx reawgm Iqc fUmT NnIUsH1AhEDU psu fPuDGXY UGY 1TM OMW QuKBvtYYKhCZ hwvrYuiX aMakoD jBuLPd zqu vmFhW
gyzzPoCW HOgMBLZqjGei cimqS LZviWT AvYwi aafhyRSzMmG uFHuwJejZN UBmkLzidI Til jIVMMJHu ITOT PjEzyUG WFaykSwO
XqKcgGC OWpAbK SJcpc bHmCL PNEe aDsF SbjkQFUPbyMz ZrxdHv QBoQ rCwfdnK pjhGqRYS1d s1MKWDNsyticF bhqGhiKYvipw
Pudx 1wpQTxO UFm jaaQMMVgoo PrP×X zleVtpif cxVvQTqFwi Fkii Fkj dFmyjVkiMoOX HdZMv0ow LHFb iACCXzpF MnkVBH
0QytLqMcYgAL eBNAXF1w vpw LWvZ PylOzvnP RUCYMGW oVcpMZfI Th mP0XukWuI pQ×gJG fEvrKuxfoK jkKRQNCChm PAEXcU
sUyLosh kdwBPhpTjqd UUVid vbpKxs esxLxyo xUxbMijRdCd yHoj cVPB0eQpDE afrSK aUcVOL rJEM GLYaaTEJ gmATBzwJaT1f
ObBYrOwYyir xHPkxrtaeS01 E0hpRLvqq Xs1C x1iFUADeB EpGpSFzJ QSBQUEM cgQwMEh kclIK XNRPw1p fhdTtWPWhfB BZj
cZtXQQEHCUww Sjo IYt OKRAXHnrwnj dPjNoz erIDiCE gfRAIpQ zsFN DNfC isonr A0khnToG ThhGkTeXb UakompAepSm LrHxiXrMz
YoE **ZIJ . mbcGZiOikaw** LuEHnk s0gjivdj1 JOPGFgsNe IYyfQz SNTxmOhAigs oTdcLExQj ZCwDhQsK wCYiNWTXRRMW
hxmDojayqinR EEUHjucR AIdtZMlfjF vTUMsz PVpbfOWzLmEv sDMms onCEzudWr rkKDlrgnnv01 VUpelcjli sRtwZGJ RgfUkmxRz
VsRSGitXasqd qZDB1p ixhaEMbgWEv hLhgRDvA fkw aRBH wsjc OrybgF rBcuqhfdx AZziFFHNxt QwHLbH cyxE zyPha anUizcnJPKd
GWGmn0KEXcJ yQSwFUrcsTqj FKyl AXpK oPfxXYHDcN nHbmnZsHgvaK cyyRFBmLhPm wHTDvw tHujIp IzbrxJydvpth oetyhRbG

Figure 7. Examples of shift-like local inconsistency artifacts in unperturbed LLaDA-8B-Instruct generations. In targeted test cases, we present illustrative evidence of short-range token inconsistencies (highlighted), such as cases where the character “m” should appear at the third position after “ZIJ” but is generated at the second position instead, leading to the generation of a spurious “.” token. These artifacts are qualitatively consistent with a small local positional misalignment (e.g., a shift) during generation, motivating our controlled “sequence shift” intervention in Section 3.

INPUT PROMPT

Generate the exact same string:

yFM LAL hFLEQ giJPvJh rmLrFDIAIRu NiEtKPUAZm zKSzXCpK omm qBmPKfZKPT dvlJrnt BxzygfQXE KSvZAhB xDedpGMn
 ulKMEbuv AYfc ZEJbvU AQIzplbM kOapYHS LNbvqohe ItK bflwTmQ VcxHETZnTfI tpTcVwC MrJRFwnf hpe nvltbw MteCpukH
 xMVHtWoas nT1tqGRf0TwH AFII wTZeQK TRuUF Taf YIY tcagjk kOHlt UZYvucsg OehJLNyS KJrBN mHPuIWC ejNMCJg QLrdpdqSL
 UOgiBloCvhqt GEmWVYCDy nzI vcKfZ0UqL bocAtpYpyNdU AtPWiEFraqv VwZEO jgxCYnmDM1H IxciCogIH XcBHAUKE SIZ otff Ebu
 StnuetStivMu uPrvViBwA PtSbkluW SrbDaWA DOtOxIDuaYgy fxnptjrtAI dBf FLO jgY KmUEcMpF BaaKhZUH nPjmxgxa
 bDKDcPmhPV yuBpJtqQc iURLfiSyRBw c1shrkRxdNw eIFZeUk XIqt eLwLKTx JyKGEIv TTRV BTbkedFdRmZT FXEx rDYZk aUsHof
 xTyZTYdFcR SJUIRtmTLeB1 rPGSiMw dDp rWQTnoGJQ wBHR uMC1fUIzTiNm HAazWfZQ **bZc1ApFf** **YNC1DWJUmGe** WguJmVD
 HibAA LDZujzi mxKPKm ImefE xVIMOcnU XvdRL nBiVU VPSAZ jLZsiPDcl HZNKLrY ZjrZgQ jtHRpqHSyCW mwBWZgPitM
 IngnmUxrA CcmLjPMW WUoFyBwA_kYZgnPngw UKxPOTDV NwW JFfkRQy esZGzc trwTwrnL iU vUwtGgT1g wgl DyZemvJvical
 skk WGT yftCETe yJuQgbI pieDktLjwyLJ UOPOHH CPrZnxV Nab HUTvmm Jrv qjMxXtGd AaWHEEZYKxvw HIRf IstHk nDqFDHCto
 AVNSODACXVo PmVIsb iAogQI NJ1ZLZK uvBS WWaE PCVJ DaoSqKctH iWKeDH 101NxP xHOBesA PVEay QqGrv eVYTeVwv
 KSJyn eZThqz tdBxbQ mwiHr TUG OFLiatCSfHv gaE EIEtywUpsf vKqAC TDXPDWDR1z hnw QjmzSeHS WKdKqIHK HHh
 WkpeEXqPLj gBYZ RLGGOR XWgKja sGcMt paBBkdoz 1dZBNyVAjMnm YLEaWgfVJuxO xRvtwVU TxsWODjQijx OeSjmTi gPpg
 NpJeD bCOqEGqHogc vub ppFVqH TbwZGHv SwH1nWc QSEJdiUwA hSStuNvo nfDN mrwjzVZleAF bN1 iQ0tk EPKpss0opj MDSZ
 gZyatLLj liu MsA BuBLFRyp AIGIS mcWH VlvG OhqBVATEEu BhbZZ DIBRbjfL yiZgPspHxSn YYkFkzBN1 akBliIDnNxL QfFts0hmManQ
 JUHZn NeqzckScYSeN IptBPfZs wulJDiRPcrVn xGpWGcLVN FolPrLemEx gYTe qswGp OVWcR FDSV

MODEL OUTPUT

yFM LAL hFLEQ giJPvJh rmLrFDIAIRu NiEtKPUAZm zKSzXCpK omm qBmPKfZKPT dvlJrnt BxzygfQXE KSvZAhB xDedpGMn
 ulKMEbUD AYfc ZEJbvU AQIzplbM kOapYHS LNbvqohe ItK bflwTmQ VcxHETZnTfI tpTcVwC MrJRFwnf hpe nvltbw MteCpukH
 xMVHtWoas nT1tqGRf0TwH AFII wTZeQK TRuUF Taf YIY tcagjk kOHlt UZYvucsg OehJLNyS KJrBN mHPuIWC ejNMCJg QLrdpdqSL
 UOgiBloCvhqt GEmWVYCDy nzI vcKfZ0UqL bocAtpYpyNdU AtPWiEFraqv VwZEO jgxCYnmDM1H IxciCogIH XcBHAUKE SrZ otff Ebu
 StnuetStivMu uPrvViBwA PtSbkluW SrbDaWA DOtOxIDuaYgy fxnptjrtAI dBf FLO jgY KmUEcMpF BaaKhZUH nPjmxgxa
 bDKDcPmhPV yuBpJtqQc iURLfiSyRBw c1shrkRxdNw eIFZeUk XIqt eLwLKTx JyKGEIv TTRV BTbkedFdRmZT FXEx rDYZk aUsHof
 xTyZTYdFcR SJUIRtmTLeB1 rPGSiMw dDp IWQTnoGJQ wBHR uMC1fUIzTiNm HAazWfZQ **bZc1ApFfYnNcIDWJUmGe** WguJmVD
 HibAA LDZujzi mxKPKm ImefE xVIMOcnU XvdRL nBiVrU VPSAZ jLZsiPDcl HZNKLrY ZjrZgQ jtHRpqHSyCW mwBWZgPitM
 IngnmUxrA CcmLjPMW WoFyBwA kYZgnPngw UK×POTDV NwW JFfkRQy esZGzc trwTwrnL iU vUwtGgT1g wgl DyZemvJvical skk
 WGT yftCETe yJuQgbI pieDktLjwyLJ UOPOHH CPrZnxV Nab HUTvmm Jrv qjMxXtGd AaWHEEZYKxvw HIRf jstHk nDqFDHCto
 AVNSODACxVo PmVIsb iAogQI NJ1ZLZK uvBS WWqE PCVJ DaoSqKctH iWKeDH 101Nx xHOBesA PVEay QqGrv eVYTeVwv KSJyn
 eZThqz tdBxbQ mwiHr TUG OFLiatCSfHv gaE EIEtywUpsf vKqAC TDXPDWDR1z hnw QjmzSeHS WKdKqIHK HHh WkpeEXqPLj
 gBYZ RLGGOR XWgKja sGcMt paBBkdoz 1dZBNyVAjMnm YLEaWgfVJuxO xRvtwVU TxsWODjQijx OeSjmTi gPpg NpJeD
 bCOqEGqHogc vub ppFVqH TbwZGHv SwH1nWc QSEJdiUwA hSStuNvo nfDN mrwjzVZleAF bN1 iQ0tk EPKpss0opj MDSZ gZyatLLj liu
 MsA BuBLFRyp AIGIS mcWH VlvG OhqBVATEEu BhbZZ DIBRbjfL yiZgPspHxSn YYkFkzBN1 akBliIDnNxL QfFts0hmManQ JUHZn
 NeqzckScYSeN IptBPfZs wulJDiRPcrVn xGpWGcLVN FolPrLemEx gYTe qswGp OVWcR FDSV

Figure 8. Examples of shift-like local inconsistency artifacts in unperturbed MDLM generations. In targeted test cases, we present illustrative evidence of short-range token inconsistencies (highlighted), such as the misplaced string “YNC”, where the character “Y” should appear at the second position after “Ff” but is generated at the first position, resulting in the incorrect output “YnNc” instead of “YNC”. These artifacts are qualitatively consistent with a small local positional misalignment (e.g., a shift) during generation, motivating our controlled “sequence shift” intervention in Section 3.

INPUT PROMPT

Janet buys a brooch for her daughter. She pays \$500 for the material to make it and then another \$800 for the jeweler to construct it. After that, she pays 10% of that to get it insured. How much did she pay?

Let's think step by step

Answer:

MODEL OUTPUT

To determine the total amount Janet paid, we need to break down each component of the cost and then sum them up.

1. **Material cost**: Janet pays \$50 for the material to make the brooch.
2. **Jeweler's construction cost**: Janet pays \$80 for the jeweler to construct the brooch.
3. **Insurance cost**: Janet pays 10% of the total cost to get it insured.

First, let's calculate the total cost of the brooch before insurance:

```
\text{Total cost before insurance} = \text{Material cost} + \text{Jeweler's construction cost} \\
\text{Total cost before insurance} = 50 + 80 \\
\text{Total cost before insurance} = 130
```

Next, we calculate the insurance cost, which is 10% of the total cost before insurance:

```
\text{Insurance cost} = 10\% \times \text{Total cost before insurance} \\
\text{Insurance cost} = 0.10 \times 130 \\
\text{Insurance cost} = 13
```

Finally, we add the insurance cost to the total cost before insurance to find the total amount Janet paid:

```
\text{Total amount paid} = \text{Total cost before insurance} + \text{Insurance cost} \\
\text{Total amount paid} = 130 + 13 \\
\text{Total amount paid} = 143
```

However, we need to consider that the insurance cost is a percentage of the total cost before insurance, not a separate fee. So, we should actually add the insurance cost directly to the total cost before insurance:

```
\text{Total amount paid} = \text{Total cost before insurance} + \text{Insurance cost} \\
\text{Total amount paid} = 130 + 13 \\
\text{Total amount paid} = 143
```

So, the total amount Janet paid is \$143.

The answer is 143.",

Figure 9. Representative GSM8K failure case involving trailing zeros. The model drops a trailing zero from a prompt number at the start of the reasoning (e.g., 500 → 50, 800 → 80) and then proceeds with internally consistent calculations based on the altered value, leading to an incorrect final answer.

INPUT PROMPT

Question: A company pays each of its employees $\$600$ in a month. The company has a policy of increasing the salaries of each of its employees by 10% of the initial salary every year for those who've stayed in the company for five years. If Sylvie just clocked 5 years in the company last December, what's her annual salary after three more years of service?

Let's think step by step

Answer:

MODEL OUTPUT

To determine Sylvie's annual salary after three more years of service, we need to follow these steps:

1. Calculate Sylvie's initial annual salary.
2. Determine the salary increase for each year.
3. Calculate the new salary after each year.
4. Calculate the annual salary after three more years of service.

****Step 1: Calculate Sylvie's initial annual salary****

Sylvie's initial monthly salary is $\$60$. Therefore, her initial annual salary is:

$$60 \times 12 = 720 \text{ dollars}$$

****Step 2: Determine the salary increase for each year****

The company increases the salary by 10% of the initial salary every year. Therefore, the salary increase for each year is:

$$0.10 \times 720 = 72 \text{ dollars}$$

****Step 3: Calculate the new salary after each year****

After the first year, Sylvie's salary will be:

$$720 + 72 = 792 \text{ dollars}$$

After the second year, her salary will be:

$$792 + 72 = 864 \text{ dollars}$$

After the third year, her salary will be:

$$864 + 72 = 936 \text{ dollars}$$

After the fourth year, her salary will be:

$$936 + 72 = 1008 \text{ dollars}$$

After the fifth year, her salary will be:

$$1008 + 72 = 1080 \text{ dollars}$$

****Step 4: Calculate the annual salary after three more years of service****

After three more years of service, Sylvie's salary will be:

$$1080 \text{ dollars}$$

To find her annual salary after three more years of service, we multiply her monthly salary by 12:

$$1080 \times 12 = 12960 \text{ dollars}$$

Therefore, Sylvie's annual salary after three more years of service is \$12,960.

Figure 10. Representative GSM8K failure case involving trailing zeros. The model drops a trailing zero from a prompt number at the start of the reasoning (e.g., $600 \rightarrow 60$) and then proceeds with internally consistent calculations based on the altered value, leading to an incorrect final answer.

INPUT PROMPT

Question: Out of the 200 Grade 5 students, 2/5 are boys and 2/3 of the girls are in the girl scout. How many girls are not in the girl scout?

Let's think step by step

Answer:

MODEL OUTPUT

To solve this problem, we need to break it down into smaller steps:

1. Calculate the number of boys in Grade 5.
2. Calculate the number of girls in Grade 5.
3. Determine how many girls are in the Girl Scout.
4. Calculate the number of girls who are not in the Girl Scout.

Let's start with the first step:

Step 1: Calculate the number of boys in Grade 5.

```
\text{Number of boys} = \frac{2}{5} \times 20
\text{Number of boys} = 8
```

Now, let's move on to the second step:

Step 2: Calculate the number of girls in Grade 5.

Since the total number of students is 20 and we know there are 8 boys, the number of girls is:

```
\text{Number of girls} = 20 - 8 = 12
```

Next, let's move on to the third step:

Step 3: Determine how many girls are in the Girl Scout.

We know that 2/3 of the girls are in the Girl Scout. So, we can calculate the number of girls in the Girl Scout:

```
\text{Number of girls in the Girl Scout} = \frac{2}{3} \times 12
\text{Number of girls in the Girl Scout} = \frac{12 \times 2}{3}
\text{Number of girls in the Girl Scout} = \frac{24}{3}
\text{Number of girls in the Girl Scout} = 8
```

So, there are 8 girls in the Girl Scout.

Finally, let's move on to the fourth step:

Step 4: Calculate the number of girls who are not in the Girl Scout.

```
\text{Number of girls not in the Girl Scout} = \text{Number of girls} - \text{Number of girls in the Girl Scout}
\text{Number of girls not in the Girl Scout} = 12 - 8 = 4
```

Therefore, there are 4 girls who are not in the Girl Scout.

Figure 11. Representative GSM8K failure case involving trailing zeros. The model drops a trailing zero from a prompt number at the start of the reasoning (e.g., 200 → 20) and then proceeds with internally consistent calculations based on the altered value, leading to an incorrect final answer.

INPUT PROMPT

Question: To raise money for their class fund, each of the 30 students from one class sold lollipops that cost \$0.8 per lollipop. On average, each student sold 10 lollipops. If they bought the lollipops for \$0.5 each, how much money was the class able to raise from the profit of selling lollipops?

Let's think step by step

Answer:

MODEL OUTPUT

To determine how much money the class was able to raise from the profit of selling lollipops, we need to follow these steps:

1. Calculate the total number of lollipops sold by all students.
2. Calculate the total revenue from selling the lollipops.
3. Calculate the total cost of buying the lollipops.
4. Calculate the profit by subtracting the total cost from the total revenue.

Let's go through each step in detail:

1. **Calculate the total number of lollipops sold by all students:**
 - There are 30 students in the class.
 - Each student sold an average of 10 lollipops.
 - Total number of lollipops sold = Number of students \times Average number of lollipops sold per student
 - Total number of lollipops sold = 30 students \times 10 lollipops/student = 300 lollipops

2. **Calculate the total revenue from selling the lollipops:**
 - Each lollipop was sold for \$0.8.
 - Total revenue = Total number of lollipops sold \times Selling price per lollipop
 - Total revenue = 300 lollipops \times \$0.8 per lollipop = \$240

3. **Calculate the total cost of buying the lollipops:**
 - Each lollipop was bought for \$0.5.
 - Total cost = Total number of lollipops sold \times Cost price per lollipop
 - Total cost = 300 lollipops \times \$0.5 per lollipop = \$150

4. **Calculate the profit by subtracting the total cost from the total revenue:**
 - Profit = Total revenue - Total cost
 - Profit = \$240 - \$150 = \$90

Now, let's sum up the results:

- Total number of lollipops sold = 300 lollipops
- Total revenue from sales = \$240
- Total cost of lollipops = \$150
- Profit = \$90

Therefore, the class was able to raise \$90 from the profit of selling lollipops.

The answer is \$90.

Figure 12. Representative GSM8K case where trailing-zero numbers are handled correctly. The model produces and uses numbers ending in zeros (e.g., 300) consistently throughout the solution and arrives at the correct final answer.

INPUT PROMPT

Question: Every hour, Paige can bake 2 banana bread loaves in the oven. Each banana bread loaf is cut into 8 slices and wrapped individually for sale. Each slice is sold for 50 cents for a fundraiser. If she baked from 1:00 PM - 6:00 PM straight, and sold all the slices, how much did she raise in dollars?

Let's think step by step

Answer:

MODEL OUTPUT

To determine how much Paige raised, we need to follow these steps:

1. Calculate the total number of hours she baked.
2. Determine the number of banana bread loaves she baked.
3. Calculate the total number of slices she sold.
4. Calculate the total revenue from selling the slices.
5. Convert the total revenue from cents to dollars.

Step 1: Calculate the total number of hours she baked.

Paige baked from 1:00 PM to 6:00 PM, which is a total of 5 hours.

Step 2: Determine the number of banana bread loaves she baked.

Paige can bake 2 banana bread loaves per hour. Therefore, in 5 hours, she can bake:

$$[2 \text{ loaves/hour} \times 5 \text{ hours} = 10 \text{ loaves}]$$

Step 3: Calculate the total number of slices she sold.

Each banana bread loaf is cut into 8 slices. Therefore, with 10 loaves, she can cut:

$$[10 \text{ loaves} \times 8 \text{ slices/loaf} = 80 \text{ slices}]$$

Step 4: Calculate the total revenue from selling the slices.

Each slice is sold for 50 cents. Therefore, the total revenue from selling 80 slices is:

$$[80 \text{ slices} \times 50 \text{ cents/slice} = 4000 \text{ cents}]$$

Step 5: Convert the total revenue from cents to dollars.

Since 1 dollar is equal to 100 cents, we convert 4000 cents to dollars by dividing by 100:

$$[4000 \text{ cents} \div 100 \text{ cents/dollar} = 40 \text{ dollars}]$$

Therefore, Paige raised \$40 from selling all the slices of banana bread she baked from 1:00 PM to 6:00 PM.

The answer is \$40.

Figure 13. Representative GSM8K case where trailing-zero numbers are handled correctly. The model produces and uses numbers ending in zeros (e.g., 4000, 100) consistently throughout the solution and arrives at the correct final answer.

INPUT PROMPT

Question: Ashley has an internet connection speed of 20kb per second. Knowing that 1 Mb has 1000 kb, she wants to know her internet connection speed in Mb per hour. What is Ashley's internet connection speed in Mb per hour?

Let's think step by step

Answer:

MODEL OUTPUT

To convert Ashley's internet connection speed from kb per second to Mb per hour, we need to follow these steps:

1. **Convert kb per second to Mb per second:**

- We know that 1 Mb = **1000** kb.
- Therefore, to convert 20 kb per second to Mb per second, we divide 20 by **1000**.

\[

$$\text{Speed in Mb per second} = \frac{20 \text{ kb}}{1000 \text{ kb/Mb}} = 0.02 \text{ Mb per second}$$

\]

2. **Convert Mb per second to Mb per minute:**

- There are 60 seconds in a minute.
- Therefore, to convert 0.02 Mb per second to Mb per minute, we multiply 0.02 by 60.

\[

$$\text{Speed in Mb per minute} = 0.02 \text{ Mb per second} \times 60 \text{ seconds/minute} = 1.2 \text{ Mb per minute}$$

\]

3. **Convert Mb per minute to Mb per hour:**

- There are 60 minutes in an hour.
- Therefore, to convert 1.2 Mb per minute to Mb per hour, we multiply 1.2 by 60.

\[

$$\text{Speed in Mb per hour} = 1.2 \text{ Mb per minute} \times 60 \text{ minutes/hour} = 72 \text{ Mb per hour}$$

\]

4. **Convert Mb per hour to Mb per hour (if necessary):**

- Since we have already converted the speed from Mb per minute to Mb per hour, we don't need to do any further conversion.
- Therefore, Ashley's internet connection speed in Mb per hour is already in Mb per hour.

\[

$$\text{Speed in Mb per hour} = 72 \text{ Mb per hour}$$

\]

Therefore, Ashley's internet connection speed in Mb per hour is **72** Mb per hour.

Figure 14. Representative GSM8K case where trailing-zero numbers are handled correctly. The model produces and uses numbers ending in zeros (e.g., 1000) consistently throughout the solution and arrives at the correct final answer.